Quantum Electronics **45** (6) 503 – 507 (2015)

LASERS

PACS numbers: 42.55.Rz; 42.60.Jf; 42.60.Da
DOI: 10.1070/QE2015v045n06ABEH015733

Formation of a spatial laser-beam profile in a channel of high-power neodymium facilities

S.A. Bel'kov, I.N. Voronich, S.G. Garanin, B.G. Zimalin, A.V. Savkin, O.A. Sharov

Abstract. **A system for one-dimensional spatial profiling of a laser beam is suggested, capable of compensating for the spatial laser-beam distortions that arise due to a nonuniform gain distribution over the aperture in the amplifying channel of high-power Nd : glass lasers with wide-aperture stages on disk active elements. The principle of operation, the approach to calculation of the key element parameters, and calculation and experimental results of studying the formation of spatial profiles of the laser beam intensity at the output from the system in question are described. Possible applications of the system both in single-beam and multi-beam optical schemes are considered.**

Keywords: *single-coordinate beam profiling, polarisation, phase plate, beam matrix, disk amplifier.*

1. Introduction

The main amplifying channel of most modern Nd : glass laser facilities intended for studying controlled fusion comprises wide-aperture amplifying cascades based on disk active elements (AEs) [1, 2]. As a rule, the disks have the form of rectangular plates placed at the Brewster angle relative to the radiation passing through the cascade. The employment of disk cascades in the main amplifying channel of multipass laser systems makes it possible to substantially increase the aperture of the amplified beam and, as a sequence, increase the output radiation energy of the facility to a megajoule level [3]. A drawback of disk cascades is the formation of the gain that is nonuniform over the aperture, which distorts the initially uniform spatial profile of beam intensity. The nonuniformity of the gain arises due to the release of stored energy through superluminescence, which most intensively occurs along a major side of a rectangular AE [4]. Within a single AE, the gain nonuniformity can be scarcely observed. However, the power channel of high-power laser systems comprises dozens of AEs and, as a rule, operates in a multipass regime; hence, the resulting distortions of the spatial beam profile become substantial.

In the amplifier, beam distortions can be compensated for by prescribing a special shape of the beam spatial structure at the power channel input. It was shown [4, 5] that at the input of the power channel with cascades on disk AEs, the compensating beam profile should be a parabola extended along one coordinate with a minimal-to-maximal intensity ratio equal to approximately 0.35. The two-dimensional and three-dimensional spatial beam profiles presented in [4, 5] are shown in Fig. 1.

The compensating profile (Fig. 1) is formed by using a special filter with an optical density varying over the aperture, which is made by depositing a thin chromium layer of variable thickness on a surface of a transparent substrate [5]. Such

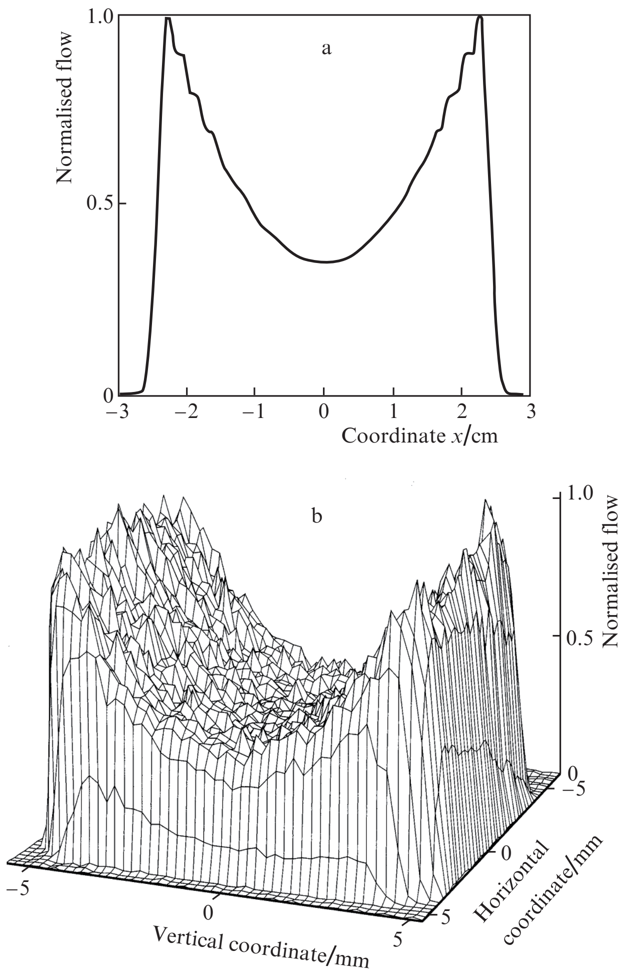

Figure 1. (a) Two-dimensional and (b) three-dimensional spatial profiles of the beam intensity at the input of a power channel of a Nd:glass laser [4, 5].

S.A. Bel'kov, I.N. Voronich, S.G. Garanin, B.G. Zimalin, A.V. Savkin, O.A. Sharov Russian Federal Nuclear Center 'All-Russian Research Institute of Experimental Physics', prosp. Mira 37, 607190 Sarov, Nizhnii Novgorod region, Russia; e-mail: voronich@otd13.vniief.ru

Received 18 December 2014; revision received 2 February 2015
Kvantovaya Elektronika **45** (6) 503 – 507 (2015)
Translated by N.A. Raspopov

filters have a number of serious drawbacks. First, it is impossible to vary the shape of the spatial beam profile with a single filter (profile correction requires producing a new filter). Second, thin-film coatings exhibit low radiation resistance, which strongly limits possible applications of such filters in channels of high-power laser facilities.

Most known systems for forming spatial beam profiles, which have high radiation resistance are either intended for forming axially symmetric profiles or cannot tune the profile without changing key optical elements [6].

A particular class of systems is based on aperture transformation of beam polarisation by phase plates with the following selection of polarisation. The phase plates in such units are usually plano-spherical lenses [4, 7] and the beam profile obtained is axially symmetric as well.

In the present work we suggest the original system [8] for one-dimensional forming and controlling the laser-beam profile (without replacing optical elements), which provides compensation for the spatial nonuniformities introduced by the gain, which is not uniform over the aperture, in the power channel of high-power Nd : glass laser facilities with cascades on wide-aperture disk AEs. The principle of operation of this system is based on nonuniform aperture transformation of the polarisation of initial radiation by a certain law with the following selection of the output beam polarisation. The key element of the system is a birefringent plane-parallel plate placed between lenses of a telescope.

2. Principle of forming the spatial beam profile

An optical scheme of the system suggested for forming the spatial laser-beam profile [8] is shown in Fig. 2.

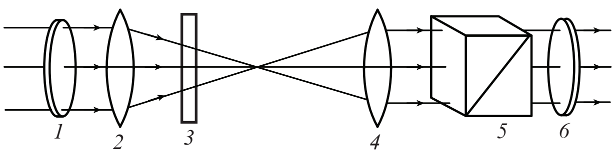

Figure 2. Optical scheme of the system for forming the spatial intensity profile of the laser beam:
(*1*, *6*) half-wave phase plates; (*2*, *4*) telescope lenses; (*3*) phase plate; (*5*) polariser.

A linearly polarised beam passes to the input of the scheme and after a telescope lens (*2*) transforms to a cone of rays falling onto the surface of a phase plate (*3*) at various angles. In the birefringent medium of the phase plate (*3*) the falling rays split to ordinary and extraordinary rays and propagate across the medium at different phase velocities. Dependence of the refractive index of the extraordinary wave on the angle between the wave vector and optical axis of the crystal (z axis) results in that for the rays with different incident angles in different planes the conditions for changing the refractive index of the extraordinary wave are not equal; consequently, the polarisation states of radiation after the phase plate also differ. A polariser (*5*) placed after the telescope lens (*4*) transforms the polarisation difference to intensity variation.

Let us now calculate the spatial profile of beam intensity at the output from the polariser for the scheme shown in Fig. 2. We introduce the coordinate system XYZ such that the phase plate will be in the plane XY (Fig. 3).

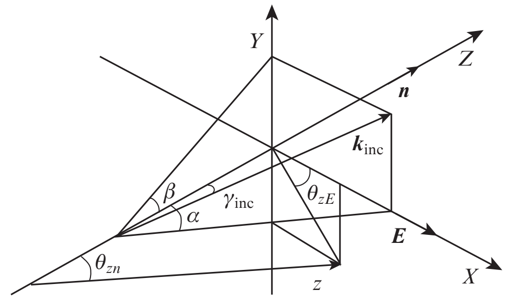

Figure 3. Positions of the polarisation vector $\boldsymbol{E}$, wave vector of incident beam $\boldsymbol{k}_{\rm inc}$, z axis of the phase plate, and normal $\boldsymbol{n}$ to its surface in the system of coordinates XYZ.

Let some ray linearly polarised in the plane XZ fall onto the surface of the phase plate at an angle $\gamma_{\rm inc}$ with the projections of the wave vector $\boldsymbol{k}_{\rm inc}$ to the planes XZ and YZ subtending with the Z-axis angles α and β, respectively. Let θ_{zn} be the angle between the z axis of the phase plate and normal $\boldsymbol{n}$ to its surface. We will calculate the radiation intensity at the output from the polariser by using the Jones matrix method [9]. The transmission plane of the polariser at the output from the phase plate is parallel to the X axis. Then the radiation intensity at the output from the polariser is given by the expression

$$I_x = C^4 + S^4 + 2C^2S^2\cos\delta, \quad (1)$$

where $C = \cos\theta_{zE}$; $S = \sin\theta_{zE}$; θ_{zE} is the angle between the projection of the z axis of the phase plate to the plane XY and the vector of polarisation $\boldsymbol{E}$ of initial radiation; and δ is the phase difference between the ordinary and extraordinary rays.

One can see from (1) that the intensity of the radiation passed through the polariser depends on the phase difference between ordinary and extraordinary rays, which, according to [10] is given by the expression:

$$\delta = \frac{2\pi}{\lambda}\Big[\frac{h}{\cos\gamma_{\rm refr}^{\rm o}}n_{\rm o} - \frac{h}{\cos\gamma_{\rm refr}^{\rm e}}n_{\rm e} + h\sin\gamma_{\rm inc}(\tan\gamma_{\rm refr}^{\rm e} - \tan\gamma_{\rm refr}^{\rm o})\Big], \quad (2)$$

where λ is the radiation wavelength; h is the plate thickness; $\gamma_{\rm refr}^{\rm o}$ and $\gamma_{\rm refr}^{\rm e}$ are the angles of refraction for the ordinary and extraordinary rays, respectively; $n_{\rm o}$ is the refractive index of the ordinary wave; and $n_{\rm e}$ is the refractive index of the extraordinary wave, which depends on the ray propagation direction in the phase plate.

By formula (1) taking into account (2) we have calculated the spatial intensity profile of the beam with a square aperture at the output from the polariser for various angles θ_{zE}. The polarisation plane, the plane of polariser transmission, and the X-axis of the coordinate system were taken parallel to each other and rotated simultaneously.

Figure 4a shows the intensity pattern with the spatial profile at the polariser output calculated for the phase plate made of a 1.5-mm-thick BBO crystal ($n_{\rm o}$ = 1.6551, $n_{\rm e}$ = 1.5426) at the angle θ_{zE} = 28.4°; the z axis of the phase plate lies in the XY plane and is parallel to horizontal sides of the square aperture of the initial beam (θ_{zn} = 90°). The radiation wave-

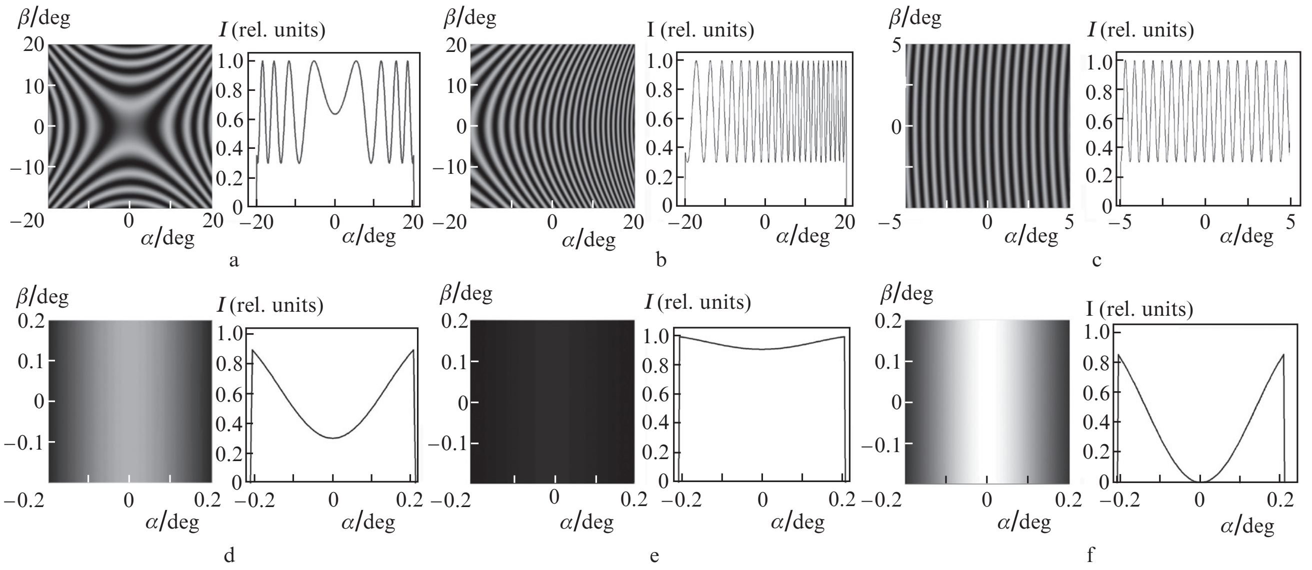

Figure 4. Calculated intensity patterns with the spatial profiles at the polariser output at the angles θ_{zE} and θ_{zn} equal to (a) 28.4° and 90°, (b) 28.4° and 80°, (c, d) 28.4° and 40°, (e) 9.2° and 40°, and (f) 45° and 40°.

length was taken 1053 nm. One can see that the intensity pattern represents a collection of lines with the same minimal intensity level.

In varying the angle θ_{zn} when the z axis and normal to the surface of phase plate remain in the same plane, the symmetry of the intensity pattern breaks, the lines of equal intensity get closer and their curvature reduces (Figs 4b, c). In a limited range of angles of ray incidence to the surface of the phase plate it is possible to obtain a single band with a minimal intensity at the centre of the pattern (Fig. 4d).

By simultaneously turning the polarisation plane of the beam and the plane of polariser transmission at a fixed position of the phase plate one can vary the level of minimal radiation intensity in the range from 0 to 1 relative to the maximal intensity [in the scheme in Fig. 2, the half-wave plates (*1*) and (*6*) are used for turning the polarisation plane of initial beam and returning the polarisation plane to the initial position after the beam leaves the polariser]. Intensity patterns with the spatial profiles at θ_{zE} = 28.4°, 9.2°, and 45° are presented in Figs 4d–f.

A comparative analysis of the spatial profiles presented in Figs 1 and 4d has shown that the maximal intensity deviation in some parts of the profiles is below 5%, which means that the system suggested is appropriate for forming and tuning the required spatial beam profile at the input of the power channel in high-power neodymium facilities with wide-aperture disk AEs.

The optical scheme in Fig. 2 can be supplemented with a tooth aperture diaphragm placed at the input of the scheme and with a selecting diaphragm placed in the general focal plane between the telescope lenses. Such a composition of the optical scheme will help simultaneously form the internal structure of the spatial profile, prescribe the shape and dimension of aperture, and perform beam apodization.

Note that the optical scheme presented in Fig. 2 requires stability of the radiation wavelength. For example, it was shown that a variation of the wavelength by $\Delta\lambda = \pm 1$ nm at λ = 1053 nm results in the transverse shift of the position of the minimal intensity level, at which the difference of maximal intensity levels at the aperture boundary is 10%, though these levels were initially equal. In addition, calculations performed for the phase plate made of the BBO crystal show that a similar shift of the minimal intensity level occurs under a variation of the crystal temperature by 14 °C.

Employment of wide-band radiation results in that for each spectral component the level of minimal intensity in the spatial profile shifts transversely over the beam aperture. Profiles of each spectral component make contribution into the resulting spatial profile, which, first of all, leads to changes in the maximal and minimal intensity levels, which at a wider spectrum tend to a common average value. However, calculations show that an increase in the radiation spectrum width, for example, to 5 nm, results in the change of the minimal-to-maximal intensity ratio in the beam by 4%, which can be compensated for by an additional change of angle θ_{zE}.

In some applications it may be desirable to vary the direction of the band of equal intensity over the beam aperture. In this case it is necessary, first, to turn the phase plate (*3*) by the required angle around the optical axis of the system and then calculate the angle θ_{zE} from the specified position of the z axis. Some additional possibilities of forming the spatial beam profile at the polariser output are presented in Fig. 5.

3. Spatial profile formation for several beams

The intensity pattern in Fig. 4c shows that, by specifying the corresponding range of angles of ray incidence onto the surface of the phase plate (*3*) (see Fig. 2) one can form several bands with an alternating level of equal intensity in the intensity pattern at the output from the polariser (*5*). If the initial radiation is presented as a matrix of parallel beams of specified aperture separated by a certain distance from each other, then each beam can be combined with one of such bands. In this case, a variation of the angle θ_{zE} will tune the level of minimal intensity in all the beams simultaneously.

Figure 6 presents calculated intensity patterns with the spatial profiles of a matrix comprising 16 beams formed at the polariser output at various angles θ_{zE} for the phase plate made of 5-mm-thick KDP (n_o = 1.4944, n_e = 1.46035, θ_{zE} = 43°). One can see that the minimal intensity level varies equally and

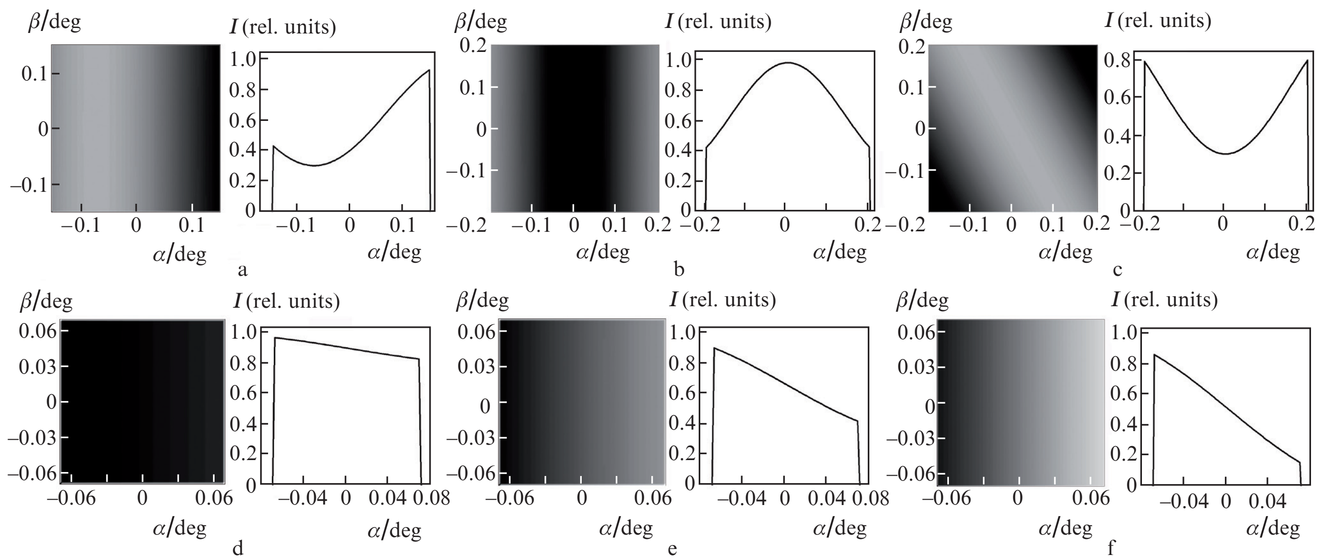

Figure 5. Calculated intensity patterns with the spatial profiles at polariser output (a, b) at an inclined phase plate, (c) in turning the phase plate around the optical axis of the system, and (d–f) in changing the angle θ_{zE} within a limited range of angles of ray incidence to the surface of the phase plate.

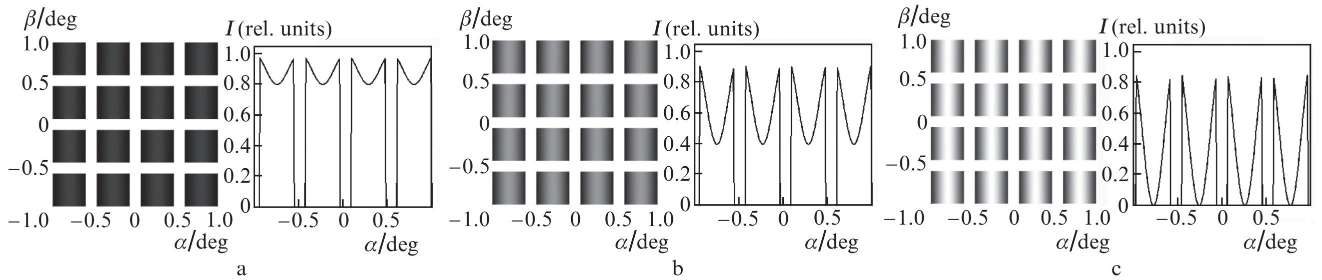

Figure 6. Intensity patterns with the intensity profiles calculated for a beam matrix at the polariser output at θ_{zE} = (a) 13.3°, (b) 25.4°, and (c) 45°.

simultaneously in all the beams; hence, the single-beam optical scheme of the system can be employed for forming the spatial profile of several beams, which may be useful in a path of multichannel laser facilities.

4. Results of experimental investigations

Experimental tryout of the system for forming the spatial beam profile was performed according to the scheme shown in Fig. 2 by using a specially formed apodized beam with a square aperture (λ = 1053 nm). In experiments with the single-beam optical scheme, the beam aperture size was 12 × 12 mm, the focal length of the first lens in the telescope was f_1 = 120 cm, the phase plate was made of a 1.5-mm-thick α-BBO crystal with the angle θ_{zn} = 40°. In experiments with the multi-beam optical scheme, the initial laser beam of size 17 × 17 mm was preliminarily separated over aperture to 16 parallel beams of size ~3.3 × 3.3 mm (with a distance between the beams of 1.3 mm) by using a matrix of diaphragms with sharp edges. A KDP crystal was used as the phase plate (with a thickness of 5 mm, θ_{zn} = 43°), f_1 = 70 cm. Experimentally measured near-field zones with the spatial beam intensity profiles at the output from the beam profile formation unit are shown for various values of angle θ_{zE} in Figs 7a–c for the single-beam scheme, and in Figs 7d–f for the case of 16 beams.

Experimental results (Fig. 7) well agree with calculations and confirm feasibility of practical realisation of the suggested system, which is capable of forming and controlling the spatial profile of single or several laser beams within wide limits. Local spatial nonuniformities of beam intensity profiles in Figs 7d–f are related to diffraction effects, which become noticeable at small dimensions of beam apertures.

5. Conclusions

An original optical scheme of the system for forming the spatial laser-beam profile intended for compensating for spatial distortions caused by a nonuniform gain distribution over the aperture in the power channel of high-power Nd : glass laser facilities with wide-aperture disk AEs is proposed, calculated, and experimentally investigated. It was demonstrated that the beam profile can be formed, which actually coincides in shape with similar beams used in modern laser facilities. An advantage of the system is the possibility to tune the shape of the spatial beam profile in wide limits without changing the optical elements. A variant of the optical scheme is suggested with a tooth aperture diaphragm, which provides simultaneous spatial profiling and apodization of the beam. The scheme based on the single-beam variant is suggested for multichannel laser systems, which can simultaneously tune the spatial profile of several laser beams. A system like this may be especially useful at a stage of commissioning high-power neodymium facilities, when try-out of various amplification regimes

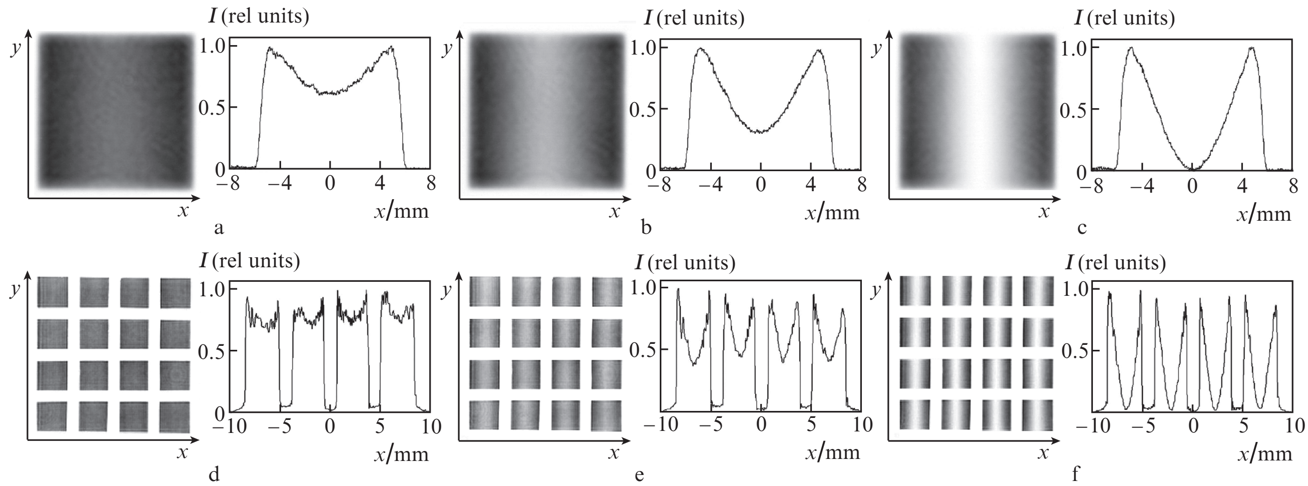

Figure 7. Experimentally measured near-field zones with the beam intensity profiles at the output from (a–c) single-beam and (d–f) 16-beam schemes of the system for spatial profiling at the angles θ_{zE} = (a) 19.6°, (b) 28.4°, (c, f) 45°, (d) 14°, and (e) 21°.

requires operative correction of the spatial intensity profile of laser beams at the input of the main amplifying channel.

References

1. Van Wonterghem B.M., Murray J.R., Campbell J.H., Speck D.R., Barker C.E., Smith I.C., Browning D.F., Behrendt W.C. *Appl. Opt.*, **36**, 4932 (1997).
2. Cavallier C., Fleurot N., Di-Nicola J-M. *Proc. SPIE Int. Soc. Opt. Eng.*, **5580**, 443 (2005).
3. Burkhart S.C., Bliss E., Di Nicola P., Kalantar D., Lowe-Webb R., McCarville T., Nelson D., Salmon T., Schindler T., Villanueva J., Wilhelmsen K. *Appl. Opt.*, **50**, 1136 (2011).
4. Van Wonterghem B.M., Salmon J.T., Wilcox R.W. *Inertial Confinement Fusion*, **5**, 45 (1995).
5. Auerbach J.M. *Inertial Confinement Fusion*, **5**, 80 (1995).
6. Mak A.A., Soms L.N., Fromzel' V.A., Yashin V.E. *Lazery na neodimovom stekle* (Neodymium Glass Lasers) (Moscow: Nauka, 1990) p.156.
7. Papernyi S.B., Serebryakov V.A., Yashin V.E. *Kvantovaya Elektron.*, **5**, 2059 (1978) [*Sov. J. Quantum Electron.*, **8**, 1165 (1978)].
8. Zimalin B.G., Savkin A.V., Sharov O.A. Patent of the Russian Federation No. 2410735, the priority of 27.01.2009.
9. Gerrard A., Burch J.M. *Introduction to Matrix Methods in Optics* (London: Wiley, 1975; Moscow: Mir, 1978).
10. Born M., Wolf E. *Principles of Optics* (London: Pergamon, 1959; Moscow: Nauka, 1973).